

Towards Automated 3D Finite Element Modeling of Direct Fiber Reinforced Composite Dental Bridge

Wei Li,¹ Michael V. Swain,^{1,2} Qing Li,³ Grant P. Steven⁴

¹ School of Aerospace, Mechanical and Mechatronic Engineering, The University of Sydney, Sydney, NSW 2006, Australia

² Faculty of Dentistry, The University of Sydney, Sydney, NSW 2006, Australia

³ School of Engineering, James Cook University, Townsville, QLD 4811, Australia

⁴ Strand 7 Pty Ltd, Suite 1, Level 5, 65 York Street, Sydney, NSW 2000, Australia

Received 23 November 2003; revised 17 October 2004; accepted 18 October 2004

Published online 23 May 2005 in Wiley InterScience (www.interscience.wiley.com). DOI: 10.1002/jbm.b.30233

Abstract: An automated 3D finite element (FE) modeling procedure for direct fiber reinforced dental bridge is established on the basis of computer tomography (CT) scan data. The model presented herein represents a two-unit anterior cantilever bridge that includes a maxillary right incisor as an abutment and a maxillary left incisor as a cantilever pontic bonded by adhesive and reinforced fibers. The study aims at gathering fundamental knowledge for design optimization of this type of innovative composite dental bridges. To promote the automatic level of numerical analysis and computational design of new dental biomaterials, this report pays particular attention to the mathematical modeling, mesh generation, and validation of numerical models. To assess the numerical accuracy and to validate the model established, a convergence test and experimental verification are also presented. © 2005 Wiley Periodicals, Inc. *J Biomed Mater Res Part B: Appl Biomater* 74B: 520–528, 2005

Keywords: CT scan; CAD; finite element; dental biomaterials; dental bridge

INTRODUCTION

One of the fundamental difficulties in the stress analysis of a dental prosthesis with new biomaterials is the highly irregular shape and intricate material properties of human tooth structure, which makes the accurate analysis very time-consuming and to a certain extent thereby minimizes the potential clinical usefulness of such an approach. In order to achieve acceptable numerical analysis accuracy, one of the effective efforts is to represent the geometry of the tooth anatomy as accurately as possible.

With the development of computer and digitizing technologies, various high-resolution inspections or shape-capturing techniques have been extensively employed recently to define the geometric surfaces of complex three-dimensional objects. From the existing literature, the following several methods are considered suitable to obtain the digitized description of the human teeth and dental bridge geometry.

Method 1: Embedding the bridge in a plastic resin, cutting and measuring serial sections^{1–4} that can provide reason-

able accuracy of information in cross-sectional geometry. However, this method is limited for the generation of very thin sections, results in destruction of the specimen, and needs considerable effort for specimen preparation and geometry digitization.

Method 2: Using the information of the average dimensions of human teeth,^{5–7} which provides a representative model, and no need to access any machines or devices. But it is hard to obtain accurate shape and geometry for individuals, and also requires considerable time and effort for sketch preparation, geometry measurement, and digitization.

Method 3: Detecting digital information of geometries based on computer tomography (CT) scan,^{8–11} which provides a higher accuracy of cross-sectional geometry and speed of digitization, fine description of the geometry, and preservation of the specimen, but needs accessing to a micro-CT scanner and some model reconstructing programs.

Compared with Method 1 (cutting, measuring, and drawing) and Method 2 (average outline drawing), the CT scanning approach is obviously more effective and promising for capturing intricate dental anatomic geometry. For this reason,

Correspondence to: W. Li (e-mail: wei@aeromuch.usyd.edu.au)

the nondestructive CT technique is adopted in this study to detect the geometry of the dental bridge model.

It is evident that from the recent literature that the CT-based FE modeling technique has been increasingly utilized for a range of biomechanical problems during the last decade, e.g., mid-cervical vertebra,¹² trabecular bone,¹³ human skull,¹⁴ limb,¹⁵ human thorax,¹⁶ human femur,¹⁷ proximal femur,¹⁸ bone microstructures,¹⁹ and so on. To make realistic use of CT scan data for dental restoration, considerable effort has been devoted recently. In 1997, the authors presented a preliminary work in 3D FE modeling of the direct fiber reinforced composite bridge, in which the geometries of the abutment and pontic were digitalized by using CT scan technology.⁸ In 2001, Verdonshot et al.⁹ developed a 3D FE modeling procedure for a human premolar based on a micro-CT data-acquisition system with a 13- μm resolution, where several material interfaces were identified. To produce the FE mesh, the preprocessor of commercial software Marc (MSC.Software, Redwood City, CA) was employed and 4 node tetrahedron elements were generated. More recently, Clement et al.¹⁰ also presented a quasi-automatic FE modeling procedure within ANSYS environment (ANSYS Inc, Canonsburg, PA) by using CT scanning data. Due to their special interest in orthodontic simulation, however, the teeth were treated as rigid bodies and the reconstruction of pulp chamber has not been taken into account. From the above work, it can be claimed that the CT-based FE modeling technique to a certain extent reflects the major trend in promoting the automatic level of dental biomechanical analysis, where highly irregular geometry, gradient material properties, multiple load cases, and complex boundary conditions often dominate the cost of accurate numerical analysis. Furthermore, the CT-based modeling technique can also provide an efficient and realistic means to *in vivo* capture of the complex geometry of human tooth anatomy in the clinic.

Over the last two decades, the development of the resin-bonded bridge technique has shown certain advantages over conventional fixed partial dentures (FPD).¹¹ One of the most extensively adopted resin-bonded structures has been the Maryland-type bridge, where either a metal or all-ceramic framework is used to retain the pontic to single or double abutments.^{11,20} Since the resin-bonded FPD has a more complicated geometry and failure mechanism in contrast to conventional FPD,^{21–23} the 3D FE method has been applied to stress analysis of Maryland bridge structures.²⁰ To accommodate the complex geometry of the Maryland bridge, Lin et al. also recently developed an elegant integrating system of the resin-bonded prosthesis modeling by making use of CT data, where the tetrahedron elements were automatically generated to enable an efficient stress analysis.¹¹

As an alternative to the Maryland bridge, the direct fiber reinforced composite bridge has a special goal in promoting a “one-appointment” technique for temporary or midterm resin-bonded bridges, which was regarded as a revolutionary solution for young patients.²⁴ It is interesting to note that the CT-based modeling approach has great potential to comply with such a special requirement that will enable a tailored

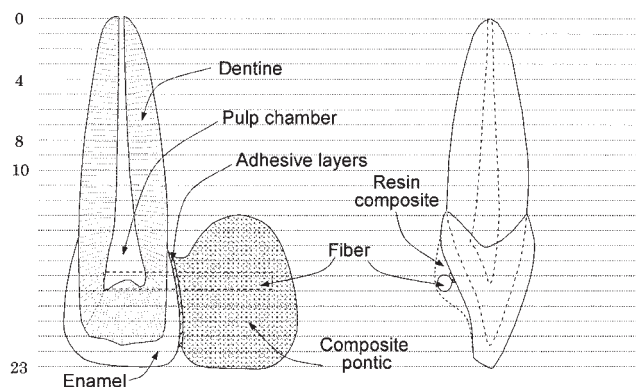


Figure 1. CT scanning sections of original dental bridge model.

design and fabrication of bridgework to individuals. In order to bring this newly emerging technique to clinical surgery, however, a great deal of work is still needed. This report aims at developing a quasi-automatic prototyping system by integrating CT scanning, image processing, CAD, in-house mesh generator, and finite element analysis (FEA). It has been noted that in the clinic, although cantilever bridges have been considerably adopted^{25,26} for (1) reducing the residual stress due to any inappropriate bridgework and (2) the unavailability of the second abutment tooth, the cantilever has been relatively less studied except with implants.^{27,28} Hence, a direct fiber-reinforced composite cantilever bridge is taken as an example to describe the modeling and validating processes in this report. Considering the bonding strength is of special significance in retaining the direct resin-bonded cantilever bridge; an approximate modeling of adhesive layer is also encompassed in FEA. The accuracy of the CT-based FE modeling is reasonably verified by a numerical convergence test and experiments.

MATERIALS AND METHODS

Physical Model of the Dental Bridge

A physical model of a two-unit cantilever dental bridge is the basis for the geometric model of the 3D finite elements in this study. As shown in Figure 1, an artificial maxillary left incisor made of composite is bonded by adhesive to a natural maxillary right incisor. The structure is reinforced by a single polyalkane fiber with a relatively high elastic modulus.

CT Scanning of the Dental Bridge Model

As a state of the art technology, a computed tomogram (CT scan) is an image produced by computer processing of data that is obtained by directing multiple narrow beams of X-ray photons through an object into detectors. The detectors measure the intensity of each beam as it emerges from the object. Each single beam, therefore, represents a measurement of the X-ray attenuation of the tissues in its path; many such paths are recorded as the X-ray tube and detectors rotate around the

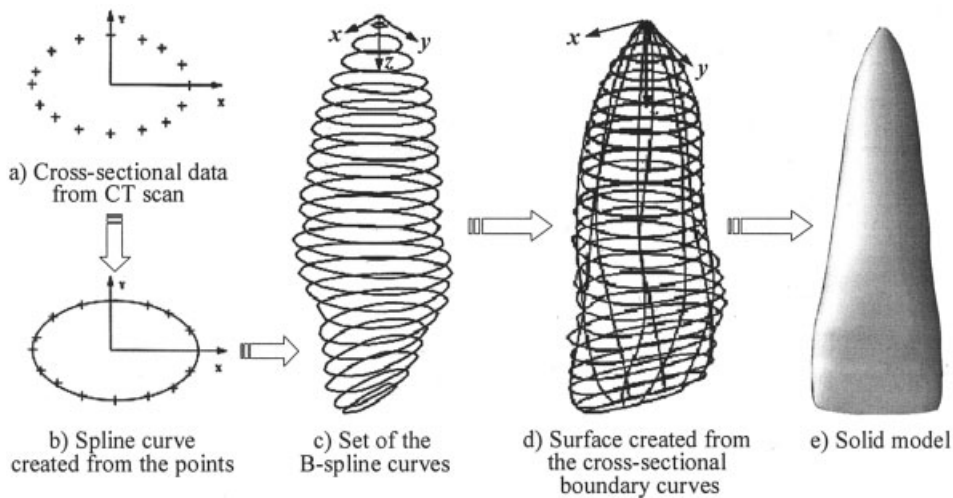


Figure 2. The procedure of reverse bioengineering within a CAD environment.

object. The computer then processes the data and mathematically superimposes all the path attenuation measurements to create an image in which the intensity at each location in the image reflects the radio intensity of that place within the object.²⁹ The pictorial arrangement of the attenuation values makes up the final CT image. The attenuation value is expressed as Hounsfield units (HU) (after one of the inventors of CT). Water has been arbitrarily assigned the value of 0 HU, with denser values ranging upward to that of bone, which can be 500 HU or more. The neighboring section of the object that is imaged with CT forms a slice with a specific thickness. If the imaged slice is conceived as a mosaic of unit volumes or voxels, the HU obtained for each voxel in the mosaic matrix can then be converted into a dot on a television screen. The brightness of each dot will depend on the density of that unit volume. The “picture” so produced is equivalent to a radiograph of that cross-sectional slice of the object.³⁰

The physical bridge model is placed in a container filled with water to attenuate the X-ray beam.²⁷ This results in a clearer image of the boundaries of the hard dental and bony tissues, since the density of water (HU = 0) more closely approximates the Hounsfield Unit for hard tissue. The images are produced using a GE9800 CT scanner in the Royal Prince Alfred Hospital, The University of Sydney. To yield a reasonable image quality for 3D reconstruction, the bridge is scanned with an interval of 1.0 mm; consequently, in total 24 serial CT sections from the abutment tooth apical root to incisal edge are acquired, as illustrated in Figure 1.

Method of Reconstructing the Structural Geometry

In general, CT scans only offer the coordinate data of cloudy scatter points in the material boundaries. These discrete points may not be suitable to directly generate FE models. Thus, various interpolation or data fitting techniques have to be employed in order to create an approximate mathematical model. Non-Uniform Rational B-Splines, known as NURBs, is one of the most popular techniques to comply with such a

computational requirement.³¹ Its high mathematical elegance and great geometric versatility have seen NURBs extensively used in various reverse engineering situations over the years. To process the CT raw data, an interface program has been developed to present the CT data to the CAD system (EDS/Unigraphics, Plano, TX) properly.

The spline curves provide an approximate interpolation based on a group of scattered points in a section. Generally speaking, spline creation may vary depending on how the sampling points are used. Shown in Figure 2 is the illustrative procedure for reconstructing a tooth profile, where only the outer surface of the dentin has been depicted. In the reconstruction of the dentin outer surface, a close spline curve is firstly fitted to the raw or extracted CT scanning points in a cross-sectional plane, as plotted in Figure 2(b). It is found that the surface construction schemes based on the blending of cross-sectional curves have a definite advantage over the point data interpolation methods as far as shape control is concerned. In other words, it appears much easier to describe a shape by using cross-sectional views than by using a cloud of scattered 3D points. More importantly, it will be seen later that this treatment is of great benefit to the development of the auto-meshing algorithm.

After the cross-sectional curves are created [Fig. 2(c)], a NURBs surface of the dentin is constructed based on those curves as illustrated in Figure 2(d). Subsequently, a solid model can be reconstructed with the help of the close NURBs surface as shown in Figure 2(e). In the exactly same way, other inner surfaces of the tooth can also be created. Finally, the entire tooth solid model is assembled by using Boolean operation, e.g., the solid of the pulp chamber is subtracted from the dentin, while the enamel is added to the dentin.

As shown in Figure 2(e), the reconstructed solid model appears highly consistent with the physical model. According to the individual dimensions, such a geometric model can be readily modified and adjusted on the basis of control parameters in the Unigraphics computer-aided design (CAD) sys-

tem used.³² Compared with the other model generation methods that were tried, it is clear that the CT scan is more time-efficient and has provided a reasonable modeling quality and efficiency.

Errors of the Geometric Model

The geometric modeling of tooth contains a set of curved surfaces that vary widely in a complex manner. It has always been difficult to describe tooth geometry exactly and completely since errors could occur in each of the methods discussed.

Firstly, errors are inevitable from digitization of the physical models due to section interval limits (24 in this study compared with 55 out of 770 in Verdonshot et al.⁹), image processing algorithm, and geometric measurements. In the reconstruction process, although current CAD platforms provide some robust tools to create free-form surfaces based on a series of scatter points, the accuracy of interpolation is still difficult to ensure particularly when the degrees of freedom of the geometric parameters are limited. The problem also happens in the areas with high curvatures, in which interpolation errors appear more nontrivial. Even with the CT scanner, some positioning errors would be introduced into the captured data.

In this case, some adjustments of reconstruction data become necessary in order to obtain a smoother curve and surface. The process is called *fairing* in CAD and reverse engineering technology. There have been different fairing methods proposed in the literature on computer-aided geometric design, but a relatively simple one is to adjust them point by point. It is worth noting that this can be very time-consuming and is carried out only when a *perfect* tooth geometry is required. In general, the geometrical modeling accuracy is reasonably acceptable compared to those resulting from FE discretization and numerical analysis.

Automated FE Mesh Generation

Compared with laboratory material testing, FEA offers a number of noteworthy advantages in parameter studies, internal stress analysis.⁹ More importantly, FEA together with CT scan, CAD/CAM, and rapid prototyping could practically enable a virtual reality and surgery plan system for the dental clinic. Without doubt, the efficiency and accuracy of the FE modeling will play a central role in the establishment of such an automated clinical procedure.

It is well known that an FE solution is greatly influenced by discretization scheme, kinematic boundaries, and load conditions. For such a complex geometry as the dental bridge, the discretization is regarded as one of the most challenge and time-consuming tasks. As a general rule, a higher order element type offers a more precise numerical solution when there is the same mesh density. On the contrary, once the type of element is chosen, a finer mesh would reduce the discretization error resulting from the replacement of a continuous structure by a discrete FE model. However, the higher order of element types and denser mesh usually increase the size of

the numerical problem (measured by degree of freedom, for short, *dof*) to be solved. Therefore, an appropriate compromise between the numerical accuracy and computing cost is necessary.

To generate FE meshes in different materials and complex geometries of dental structures, either commercial packages (e.g., Marc⁹ and ANSYS¹⁰) or in-house programs have been employed in the literature. Lin et al.¹ developed an automatic procedure of FE meshing for the second premolar. The procedure was subsequently applied to a number of interesting dental biomechanics modeling problems, e.g., mesial-occlusal-distal restoration teeth^{2,3} and cervical lesion of maxillary premolar.⁴ Nevertheless, the geometry data were acquired from the physical sliced technique (Method 1). Recently, they have attempted to integrate CT scanning into the FE modeling, where Pro/Engineer was adopted to automatically generate FE mesh for the resin-bonded Maryland-type prosthesis.¹¹ The CT-based FE modeling presented by Verdonshot et al.⁹ employed Marc to automatically generate 3D mesh from the well-represented free-form surfaces, where the 3D surfaces were firstly divided into triangles and then the volumes contained by the surfaces were divided into large number of 3D volume elements.

In the literature, it is noticed that primarily the linear tetrahedral elements have been adopted to discretize the dental structures in both the commercial and in-house mesh generators due to their flexibility in general cases. One of the main concerns with such an element type is that the boundaries of each element may be given in straight lines and, consequently, a denser mesh is usually needed to appropriately capture the freeform surfaces in dental structures. For this reason, it would be meaningful to attempt other nonlinear element types. This study demonstrates an in-house mesh generator to introduce higher order elements strategy for the discretization of the dental structures.

In the present procedure, the quadratic curved twenty-node brick elements and fifteen-node wedge elements are adopted.³³ The solid model consists of mainly brick elements as well as a few wedge elements to accommodate sharp boundary and the mesh transient of different sizes. The model is predominantly divided into five parts: abutment dentine, crown (enamel), composite pontic, reinforced fiber, and adhesive layer in abutment/pontic, abutment/fiber, and pontic/fiber interfaces. The division and interconnection of the mesh volumes as well as the subsequent subdivision of elements into brick or wedge are accomplished quasi-automatically by using the in-housing program.

Tooth dimensions differ widely from individual to individual. To have the established model more representative, proper modifications for some surface points are introduced from the drawings (Method 2) in the present example. In the real model, the fiber is covered by a resin composite to produce a smooth, convex surface (Figure 1). Since this coverage has relatively little effect on the strength of the bridge compared with the fiber, it is neglected in the FE modeling in this study.³⁴

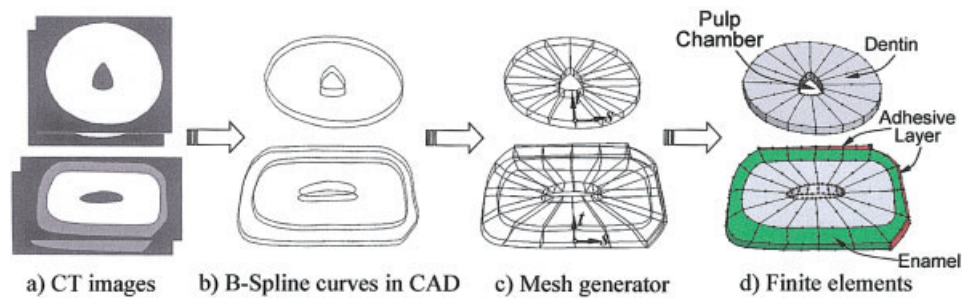


Figure 3. Procedure from CT scanning image to finite elements. [Color figure can be viewed in the online issue, which is available at www.interscience.wiley.com.]

It is evident that the root part of the abutment has a less complicated shape and a low stress concentration compared to the crown and connecting part. Thus, only a coarse mesh is arranged in the root portion whereas a dense mesh is assigned on the other parts of the bridge model. This is implemented in line with the coordinates of the longitudinal axis (along the occlusal direction), i.e., the root region (sections 0–8 in Figure 1) is meshed coarsely and the crown region (sections 11–24) is meshed densely. Sections 8–10 are set as a transient region by using the wedged elements (refer to the preliminary model shown in Figure 4).

The NURBs representation of boundary surfaces as well as solid modeling enables a flexible generation of boundary, interfacial, and internal nodes. This actually allows an arbitrary generation of brick elements over the domain. However, if one looks at the slice that is reconstructed from two consecutive CT sectional images [Figure 3(a)], the mesh generation may become simpler as in Figure 3(b,c). Figure 3 shows the meshing processes of two slices in the crown region, respectively, without and with the enamel. In the procedure, the corner nodes of the brick elements are uniformly sampled along each closed B-splined curves (in terms of curved coordinate s). Also, the corner nodes of the brick elements are created along the normal directions between these spline curves [in terms of coordinate t , as in Figure 3(c)]. The intermediate edge nodes are then generated from the curves and surfaces when located on the boundary of region/material, or from the solid model database otherwise. Also the parameters for defining mesh density, the numbers of elements along s and t , need to be prescribed beforehand.

To maintain a proper geometrical aspect ratio, a 25–100- μm -thick adhesive layer³⁵ between the abutment and pontic in the physical bridge model is modeled as a 0.2-mm-thick layer [Figure 3(d)], where slight modification (inward shrinkage in the elements connected) is introduced to allow better control of the geometry while simultaneously attempting to minimize the distortion of the mesh and thus increase the predictive accuracy of the FE model. In summary, this preliminary model consists of approximately 572 twenty-node quadratic hexahedra elements and 140 fifteen-node quadratic wedge elements with a total of 3710 nodes as shown in Figure 4. The nodal coordinates and mesh connectivity data are then transmitted into another commercial FE package Strand7

(G+D Computing, Sydney, NSW, Australia) through a special interface program between CAD and FEA platforms.

The Loading, Boundary Conditions, and Material Properties

To facilitate the convergence tests, simplified loading, boundary conditions, and material properties are applied. In the model shown in Figure 4, the bone structure that supports the root is assumed to be rigid while the periodontal ligament between the bone structure and the root is neglected. Consequently all of the root nodes, which correspond to the external surface of the root portion of dentin, are assumed to be fully fixed. A uniformly distributed bite force of total 100N is initially applied at the incisal margin of the pontic as Figure 4, but the other load cases are allowed. It is further assumed that the bite force is 26° to the longitudinal axis that represents the angle at the first contact of tooth during biting.³⁶

The materials adopted in the preliminary study include: the light-cured composite for the pontic, the adhesive for the bond, the fiber for the connector, and a human central incisor

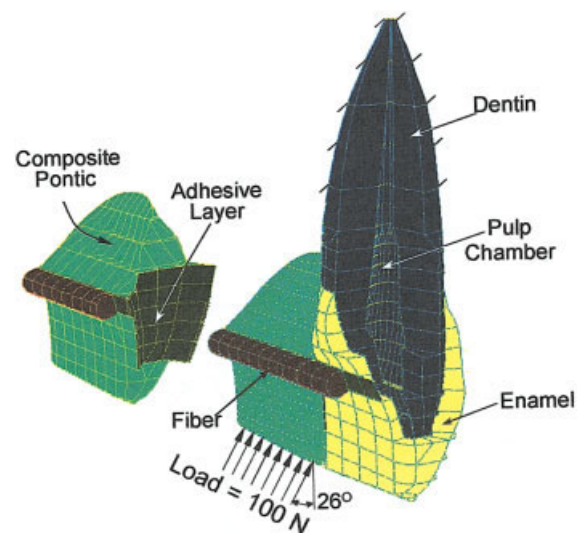


Figure 4. Finite element modeling of the bridge showing enamel, dentin, pulp regions, composite pontic, reinforced fiber, and adhesive layer. [Color figure can be viewed in the online issue, which is available at www.interscience.wiley.com.]

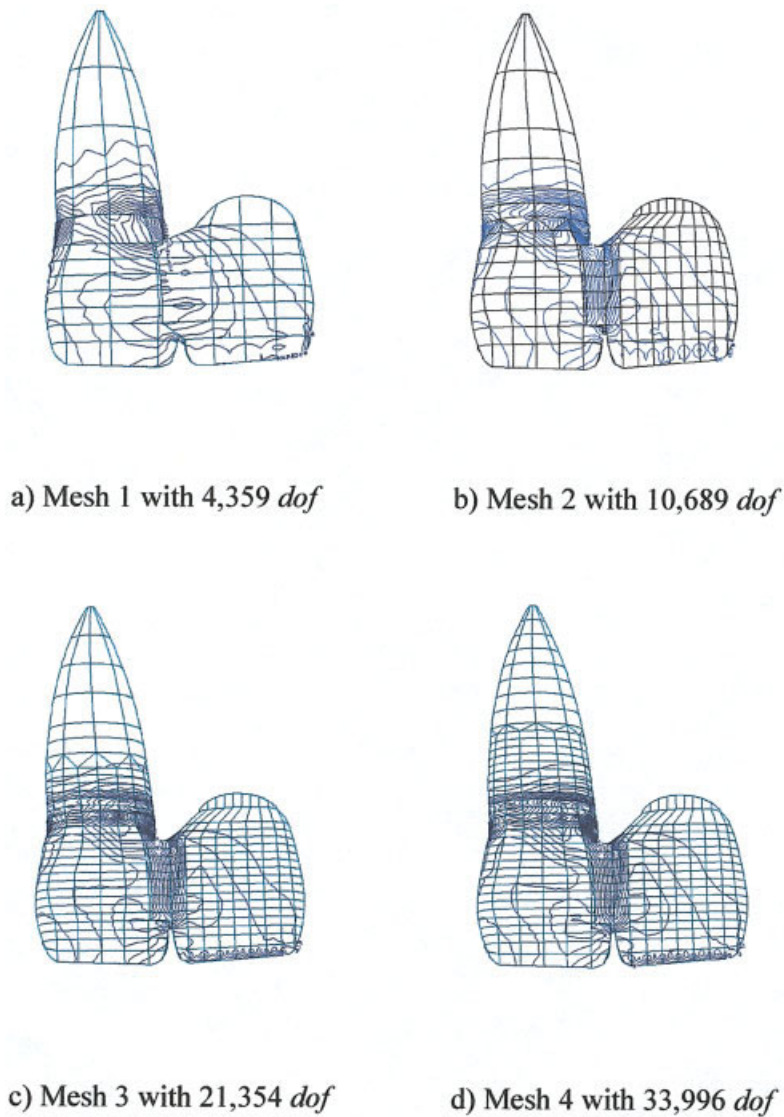


Figure 5. Refinements of 3D finite element meshes and contours of von Mises stresses. [Color figure can be viewed in the online issue, which is available at www.interscience.wiley.com.]

for the abutment. The Young's modulus of pulp is negligibly small compared to those of the enamel and dentin. Therefore, the effect of pulp on the structural analysis can be neglected and the pulp chamber is considered to be hollow. All the materials are assumed to be homogeneous, isotropic, and linear elastic. The Young's modulus³⁷ and Poisson's ratio^{37,38} of the materials are summarized in Table I.

RESULTS AND DISCUSSION

Convergence of FE Model

As pointed out earlier, the FE model replaces a physical continuum object in a discrete fashion. Theoretically, the computational result is only an approximate rather than the exact solution. Before the FE numerical result is accepted, both the accuracy and the validity of the solutions must be

objectively established.³⁹ The accuracy of FEA, i.e., measuring how well the exact solution has been approximated, can be assessed via a convergence test.¹ The validity of the solution, which measures how well the continuum has been approximated, may be determined by laboratory experiments. This study will carry out both convergence tests and laboratory experiments to verify the present CT-based FE modeling approach of the dental bridge.

TABLE I. Material Properties for the FEA Model

Material	Young's Modulus (MPa)	Poisson's Ratio
Enamel	60,000	0.33 ³⁵
Dentine	15,000	0.31 ³⁵
Fiber	50,000	0.30 ³⁴
Adhesive	2000	0.30 ³⁴
Composite	18,000	0.30 ³⁴

TABLE II. Comparison of the Maximum Tensile Stress, Specific Displacements, and Computer Time on the Four Different Meshes

	Mesh 1	Mesh 2	Mesh 3	Mesh 4
Degrees of freedom	4359	10,689	21,354	33,996
Number of nodes	1557	3710	7534	12,093
Number of elements	257	702	1418	2451
Max tensile stress σ_1 (MPa)	81.50	80.38	74.71	72.20
Max displacement u_z ($mm \times 10^{-2}$)	-4.88	-5.15	-5.21	-5.25
u_z at Point A ($mm \times 10^{-2}$)	-1.99	-2.16	-2.24	-2.32
u_z at Point B ($mm \times 10^{-2}$)	-1.29	-1.47	-1.50	-1.51
Computer time (s)	8	32	110	273

In general, the higher the order of the elements used, the better the approximation for the displacements, which is referred to as p -convergence. Also, theoretically, FE results should converge toward exact results as the mesh is refined, i.e., when more nodes and elements are properly used, the approximate solution generally improves (a process called h -convergence) and the calculated displacement at any particular node approaches the exact solution (but is generally unknown). Note that in the case of 3D analyses, each node normally has three dof representing displacements in the x , y , and z Cartesian directions. Thus, these tests can be expensive and time-consuming, and there have been very limited reports for dental bridges so far. In the study by Lin et al.,¹ the convergence test was carried out to verify the automatic meshing procedure developed, where von Mises stress contour and strain energy were checked against dof . Unfortunately, the indices of strain energies do not show a monotonic convergent pattern, but rather appeared geometry-dependent.

Considering the nature of the displacement-based FE method, the nodal displacements are selected as the convergence indices. To observe the effect of mesh density on displacements, four different meshes, with increasing numbers of nodes and elements, are generated to perform the convergence test. As in Figure 5, the mesh size varied from Mesh 1 with 257 elements (4,359 dof), Mesh 2 with 702 elements (10,689 dof), Mesh 3 with 1,418 elements (21,354 dof), to Mesh 4 with 2,451 elements (33,996 dof). All models have the same load and boundary conditions as Figure 4, as well as the same material properties as listed in Table I.

To compare detailed test results between the different mesh sizes, the tensile principal stress peaks, maximum displacements in vertical directions, displacements at specific points, and computational efficiency for these four different meshes are summarized in Table II. In all the models, it is identified that the maximum tensile stress occurs at the same position on the crown distal surface (near the cervical line of the abutment). It is also worth noting that the computing time (CPU time in a P4-1.7 GHz) varied from 8 s for Mesh 1 to 273 s for Mesh 4.

Figure 6 shows the variation of displacements at two sampled points (nodes A and B) and computing time against the number of dof . These two nodes are randomly picked from the irregularly meshed adhesive region and the largely deformed fiber region, respectively. The convergence of the

FE model is well identified from the monotonic curves. The differences between the displacements at point B are found to be approximately 0.66% between Mesh 3 and Mesh 4 (considerably smaller than 2% between Meshes 2 and 3), whereas the differences in the number of dof and computer time are 59 and 148%, respectively. In fact, the contours of the surface von Mises stresses as plotted in Figure 5 also provide further evidence of the strong similarity between Mesh 3 and Mesh 4. From the viewpoints of both accuracy and efficiency, Mesh 3 with around 21,000 degrees-of-freedom is recommended as a fundamental mesh density for further detailed numerical studies.³¹

Experimental Validation

The laboratory experiment is essential to validate the CT-based FE modeling. Based on the authors' best knowledge, however, no experimental investigation for the direct fiber dental bridge is available. As one of the primary goals of the experiment, the FE numerical results are evaluated against the test ones herein. A more thorough experimental investigation, including the failure pattern as well as the effects of design variations, parameters, and adjacent teeth, is beyond the scope of this article and is reported elsewhere.⁴⁰

Considering that the bridge stiffness is of special interest, the experiment is carried out to measure the stiffness in terms

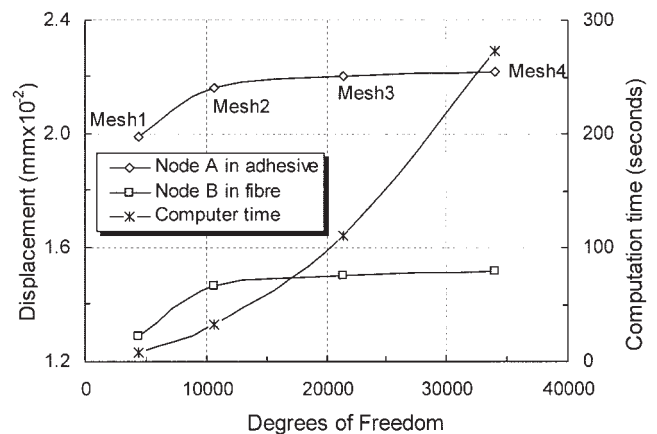


Figure 6. Nodal displacements and computing time against the number of degrees-of-freedom for the four FE meshes.

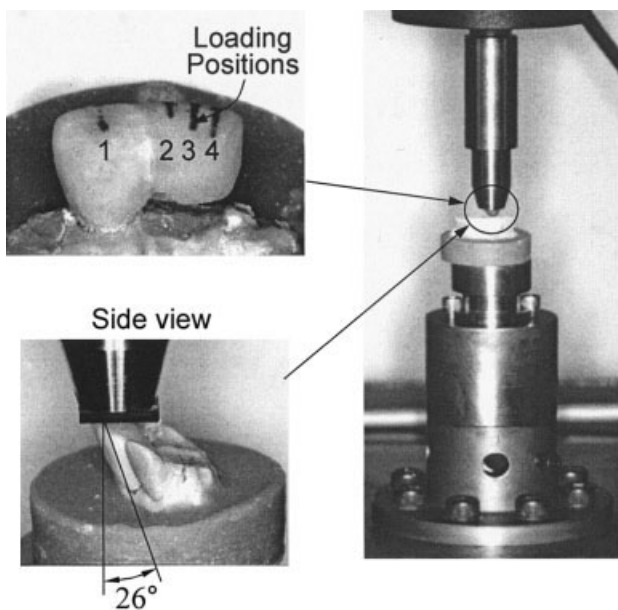


Figure 7. Detailed experimental setup for evaluating cantilever stiffness

of the slope of loading versus displacement curve, i.e., ds/dp . The overview of the experiment setup is shown in Figure 7, where the bridge specimen firmly rests on a rigid metal platform of the testing machine. To examine the stiffness more thoroughly, three specimens are prepared and four loading positions (1, 2, 3, and 4) for each specimen are set on the specimens as marked in Figure 7.

The experimental and computational stiffnesses are depicted in Figure 8. The deviations of slopes between the tests and FEA are 15, 9.9, 10.6, and 16.4% at load positions 1, 2, 3, and 4, respectively. This represents a reasonable agreement between the experimental and the predicted values when considering various sources of errors, including material properties, additional compliance associated with loading contact point jig system, and root boundary conditions of the specimens. As a result, the CT-based FE modeling is appropriately validated.

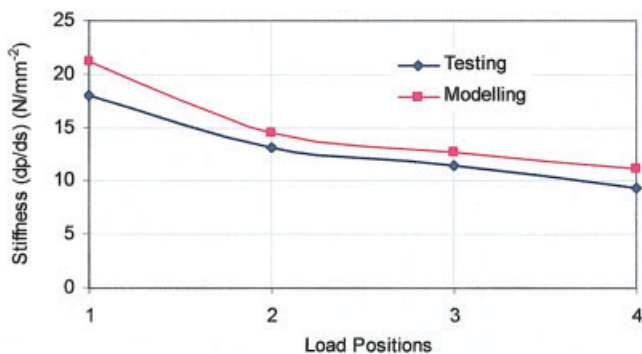


Figure 8. The experimental and numerical comparison of the dental bridge stiffness. [Color figure can be viewed in the online issue, which is available at www.interscience.wiley.com.]

CONCLUSIONS

As part of the ongoing project regarding comprehensive investigation into the direct fiber-reinforced composite dental bridge structures, this report focuses on the development of an automated procedure for FE modeling, which involves CT data processing, continuum mathematical modeling, and discretizing. The computer tomography (CT) scan technology adopted in this study seems promising for clinical dental restoration due to its nature of nondestructive detection in human teeth. It is expected that the integration of these several individual pieces of cutting-edge technologies would significantly promote the “one-appointment” technique for dental bridge production in the customized clinic.

A cloud of scatter data from the CT scanner is fitted to a continuum mathematical model in a CAD environment. Such a 3D continuum model proves to be versatile in downstream manipulations. On the basis of the mathematical model, particularly the representation of detailed CT sections, the mesh generation becomes relatively straightforward and efficient. The entire CT-based modeling procedure shows a typical example of reverse bioengineering.

The adoption of the quadratic curved elements appears suitable to describe the complex interfacial freeform surfaces in the human tooth. The adequacy of the mesh refinement in the 3D FEA model has been assessed by the implementation of convergence tests. Considering both numerical precision and computational efficiency, a FE model with over 20,000 degrees of freedom is suggested. In addition, the CT-based FE modeling technique is appropriately validated through the laboratory tests. It is claimed that the accuracy and validity of the CT-based FE modeling procedure presented are practically effective and suitable to further biomechanical analysis and design optimization of the dental bridges.

It can be noted that one of the main advantages of developing an in-house mesh generator is to accommodate a computational shape/parameter optimization for a computer-aided dental bridge design, which will consist of many iterations of FEA, numerical sensitivity analysis, and shape modification. At some stage, a remeshing process may be needed and a full control of mesh generation will be of clear benefit for this purpose. In addition, the in-house mesh generator is suitable for the anatomic similarity of human teeth as it appears more efficient and can provide an important component for developing a stand-alone computer-aided dental clinical plan software in the future.

This study has been partially supported by Nulite System International Pty Ltd. Special thanks are due to Dr. Graham Culy from The University of Melbourne for providing the original dental bridge models and Mr. Ken Tyler, Dr. Jim Ironside, and Dr. Napa Suansuwan at the Dental Biomaterial Section in the Faculty of Dentistry, The University of Sydney, for their technical assistance on the test specimen fabricating and testing.

REFERENCES

1. Lin CL, Chang CH, Cheng CH, Wang CH, Lee HE. Automatic finite element mesh generation for maxillary second premolar. *Comput Method Prog Biol* 1999;59:187–195.

2. Lin CL, Chang CH, Ko CC. Multifactorial analysis of an MOD restored human premolar using auto-mesh finite element approach. *J Oral Rehabil* 2001;28:576–585.
3. Lin CL, Chang CH, Wang CH, Ko CC. Numerical investigation of the factors affecting interfacial stresses in an MOD restored tooth by auto-meshed finite element method. *J Oral Rehabil* 2001;28:517–525.
4. Lee HE, Lin CL, Wang CH, Cheng CH, Chang CH. Stresses at the cervical of maxillary premolar — a finite element investigation. *J Dent* 2002;30:283–290.
5. Ash MM. Wheeler's atlas of tooth form, 5th ed. Philadelphia: W.B. Saunders Co; 1984.
6. Cathey GM. Dental anatomy. Chapel Hill: University of North Carolina; 1972.
7. Fuller JL, Denehy GE. Concise dental anatomy and morphology, 2nd ed. Chicago: Year Book Medical Publishers Inc; 1984.
8. Li W, Steven GP, Doube CP. Three dimensional finite element analysis for light-curved composite dental bridge. In: Middleton J, Jones ML, Pande GN, editors. Proceedings of the Third International Symposium on Computer Methods in Biomechanics and Biomedical Engineering. New York: Gordon and Breach Publishers; 1997. p 713–720.
9. Verdonschot N, Fennis WMM, Kuijs RH, Stolk J, Kreulen CM, Creugers NHJ. Generation of 3D finite element models of restored human teeth using micro-CT techniques. *Int J Prosthodont* 2001;14:310–315.
10. Clement R, Schneider J, Brambs HJ, Wunderlich A, Geiger M, Sander FG. Quasi-automatic 3D finite element model generation for individual single-rooted and periodontal ligament. *Comput Methods Prog Biol* 2003;73:135–144.
11. Lin CL, Lee HE, Wang CH, Chang CH. Integration of CT, CAD system and finite element method to investigate interfacial stresses of resin-bonded prosthesis. *Comput Methods Prog Biol* 2003;72:55–64.
12. Bozic KJ, Keyak JH, Skinner HB, Bueff HU, Bradford DS. 3-Dimensional finite-element modeling of a cervical vertebra: an investigation of burst fracture mechanism. *J Spinal Disord* 1994;7:102–110.
13. Muller R, Rueggsegger P. 3-Dimensional finite-element modeling of noninvasively assessed trabecular bone structures. *Med Eng Phys* 1995;17:126–133.
14. Krabbel G, Appel H. Development of a finite-element model of the human skull. *J Neurotrauma* 1995;12:735–742.
15. Commean PK, Smith KE, Vannier MW, Szabo BA, Actis RL. Finite element modeling and experimental verification of lower extremity shape change under load. *J Biomech* 1997;30:531–536.
16. Kinst TF, Sweeney MO, Lehr JL, Eisenberg SR. Simulated internal defibrillation in humans using an anatomically realistic three-dimensional finite element model of the thorax. *J Cardiovasc Electr* 1997;8:537–547.
17. Viceconti M, Zannoni C, Testi D, Cappello A. A new method for the automatic mesh generation of bone segments from CT data. *J Med Eng Technol* 1999;23:77–81.
18. Keyak JH, Rossi SA, Jones KA, Skinner HB. Prediction of femoral fracture load using automated finite element modeling. *J Biomech* 1998;31:125–133.
19. Borah B, Gross GJ, Dufresne TE, Smith TS, Cockman MD, Chmielewski PA, Lundy MW, Hartke JR, Sod EW. Three-dimensional microimaging (MR mu I and mu CT), finite element modeling, and rapid prototyping provide unique insights into bone architecture in osteoporosis. *Anat Rec* 2001;265:101–110.
20. Pospiech P, Rammelsberg P, Goldhofer G, Gernet W. All-ceramic resin-bonded bridges: a 3-dimensional finite-element analysis study. *Eur J Oral Sci* 1996;104:390–395.
21. Creugers NHJ, Kayser AF. An analysis of multiple failures of resin-bonded bridges. *J Dent* 1992;20:348–351.
22. Creugers NHJ, Kayser AF, Vanthof MA. A 7-1/2 year survival study of resin-bonded bridges. *J Dent Res* 1992;71:1822–1825.
23. Priest G. An 11-year reevaluation of resin-bonded fixed partial dentures. *Int J Periodont Rest Dent* 1995;15:239–247.
24. Ibsen RL. One-appointment technique using an adhesive composite. *Dent Surv* 1973;49:30–32.
25. Hammerle CHF, Ungerer MC, Fantoni PC, Bragger U, Burgin W, Lang NP. Long-term analysis of biologic and technical aspects of fixed partial dentures with cantilevers. *Int J Prosthodont* 2000;13:409–415.
26. Jepson N, Allen F, Moynihan P, Kelly P, Thomason M. Patient satisfaction following restoration of shortened mandibular dental arches in a randomized controlled trial. *Int J Prosthodont* 2003;16:409–414.
27. Young FA, Williams KR, Draughn R, Strohaber R. Design of prosthetic cantilever bridgework supported by osseointegrated implants using the finite element method. *Dent Mater* 1998;14:37–43.
28. Romeo E, Lops D, Margutti E, Ghisolfi M, Chiapasco M, Vogel G. Implant-supported fixed cantilever prostheses in partially edentulous arches. A seven-year prospective study. *Clin Oral Implant Res* 2003;14:303–311.
29. Freedman M. Clinical imaging: an introduction to the role of imaging in clinical practice. New York: Churchill Livingstone; 1988.
30. Squire LF, Novelline RA. Fundamentals of radiology, 4th ed. Cambridge, MA: Harvard University Press; 1988.
31. Choi BK. Surface modeling for CAD/CAM. New York: Elsevier Science Publisher; York; 1991.
32. EDS. Unigraphics user's manual, Version 12; Plano, TX, 1996.
33. G+D Computing. Strand7 finite element analysis system reference manual and user guide. Sydney, Australia: G+D Computing Pty Ltd; 2000.
34. Li W, Swain MV, Li Q, Ironside J, Steven GP. Fiber reinforced composite dental bridge, Part II numerical investigation. *Biomaterials* 2004;25:4995–5001.
35. Plekavich EJ, Joncas JM. The effect of impression-die systems on crown margins. *J Prosthet Dent* 1983;49:772–776.
36. Darendeliler S, Darendeliler H, Kinoglu T. Analysis of a central maxillary incisor by using a three-dimensional finite element method. *J Oral Rehabil* 1992;19:371–383.
37. Nulite. Material Test Reports. Sydney, Australia: Nulite System International Pty Ltd; 1995.
38. Farah JW, Craig RG, Meroueh KA. Finite element analysis of three- and four-unit bridges. *J Oral Rehabil* 1989;16:603–611.
39. Huiskes R, Chao EYS. A survey of finite element analysis in orthopedic biomechanics: the first decade. *J Biomech* 1983;16:385–409.
40. Li W, Swain MV, Li Q, Ironside J, Steven GP. Fiber reinforced composite dental bridge, Part I experimental investigation. *Biomaterials* 2004;25:4897–4993.